EUROPEAN ORGANIZATION FOR NUCLEAR RESEARCH

CERN-PPE/95-122
3rd August 1995

A Study of b Quark Fragmentation into B^0 and B^+ Mesons at LEP

The OPAL Collaboration

Abstract

A study of b quark fragmentation at LEP is presented using a sample of semileptonic B decays containing a fully reconstructed charm meson. The data are compared to several theoretical models for heavy quark fragmentation; the free parameters in these models are fitted and the sensitivity of the model parameters to the rate of P-wave B meson production is studied. The mean scaled energy fraction of B^0 and B^+ mesons has been determined to be $\langle x_E \rangle = 0.695 \pm 0.006 \pm 0.003 \pm 0.007$, where the errors are statistical, systematic and model dependence respectively. This result is consistent with previous, less direct measurements from inclusive leptonic B decays. Also presented is a model independent fit to the shape of the energy distribution of weakly decaying B mesons at LEP.

(Submitted to Physics Letters B)

The OPAL Collaboration

G. Alexander[23], J. Allison[16], N. Altekamp[5], K. Ametewee[25], K.J. Anderson[9], S. Anderson[12], S. Arcelli[2], S. Asai[24], D. Axen[29], G. Azuelos[18,a], A.H. Ball[17], E. Barberio[26], R.J. Barlow[16], R. Bartoldus[3], J.R. Batley[5], G. Beaudoin[18], J. Bechtluft[14], A. Beck[23], G.A. Beck[13], C. Beeston[16], T. Behnke[8], K.W. Bell[20], G. Bella[23], S. Bentvelsen[8], P. Berlich[10], S. Bethke[14], O. Biebel[14], I.J. Bloodworth[1], P. Bock[11], H.M. Bosch[11], M. Boutemeur[18], S. Braibant[12], P. Bright-Thomas[25], R.M. Brown[20], H.J. Burckhart[8], C. Burgard[27], R. Bürgin[10], P. Capiluppi[2], R.K. Carnegie[6], A.A. Carter[13], J.R. Carter[5], C.Y. Chang[17], C. Charlesworth[6], D.G. Charlton[1,b], S.L. Chu[4], P.E.L. Clarke[15], J.C. Clayton[1], S.G. Clowes[16], I. Cohen[23], J.E. Conboy[15], O.C. Cooke[16], M. Cuffiani[2], S. Dado[22], C. Dallapiccola[17], G.M. Dallavalle[2], C. Darling[31], S. De Jong[12], L.A. del Pozo[8], H. Deng[17], M.S. Dixit[7], E. do Couto e Silva[12], E. Duchovni[26], G. Duckeck[8], I.P. Duerdoth[16], U.C. Dunwoody[8], J.E.G. Edwards[16], P.G. Estabrooks[6], H.G. Evans[9], F. Fabbri[2], B. Fabbro[21], P. Fath[11], F. Fiedler[12], M. Fierro[2], M. Fincke-Keeler[28], H.M. Fischer[3], R. Folman[26], D.G. Fong[17], M. Foucher[17], H. Fukui[24], A. Fürtjes[8], P. Gagnon[6], A. Gaidot[21], J.W. Gary[4], J. Gascon[18], S.M. Gascon-Shotkin[17], N.I. Geddes[20], C. Geich-Gimbel[3], S.W. Gensler[9], F.X. Gentit[21], T. Geralis[20], G. Giacomelli[2], P. Giacomelli[4], R. Giacomelli[2], V. Gibson[5], W.R. Gibson[13], J.D. Gillies[20], D.M. Gingrich[30,a], J. Goldberg[22], M.J. Goodrick[5], W. Gorn[4], C. Grandi[2], E. Gross[26], C. Hajdu[32], G.G. Hanson[12], M. Hansroul[8], M. Hapke[13], C.K. Hargrove[7], P.A. Hart[9], C. Hartmann[3], M. Hauschild[8], C.M. Hawkes[8], R. Hawkings[8], R.J. Hemingway[6], G. Herten[10], R.D. Heuer[8], J.C. Hill[5], S.J. Hillier[8], T. Hilse[10], P.R. Hobson[25], D. Hochman[26], R.J. Homer[1], A.K. Honma[28,a], D. Horváth[32,c], R. Howard[29], R.E. Hughes-Jones[16], D.E. Hutchcroft[5], P. Igo-Kemenes[11], D.C. Imrie[25], A. Jawahery[17], P.W. Jeffreys[20], H. Jeremie[18], M. Jimack[1], A. Joly[18], M. Jones[6], R.W.L. Jones[8], U. Jost[11], P. Jovanovic[1], J. Kanzaki[24], D. Karlen[6], K. Kawagoe[24], T. Kawamoto[24], R.K. Keeler[28], R.G. Kellogg[17], B.W. Kennedy[20], B.J. King[8], J. King[13], J. Kirk[29], S. Kluth[5], T. Kobayashi[24], M. Kobel[10], D.S. Koetke[6], T.P. Kokott[3], S. Komamiya[24], R. Kowalewski[8], T. Kress[11], P. Krieger[6], J. von Krogh[11], P. Kyberd[13], G.D. Lafferty[16], H. Lafoux[21], R. Lahmann[17], W.P. Lai[19], D. Lanske[14], J. Lauber[15], J.G. Layter[4], A.M. Lee[31], E. Lefebvre[18], D. Lellouch[26], J. Letts[2], L. Levinson[26], C. Lewis[15], S.L. Lloyd[13], F.K. Loebinger[16], G.D. Long[17], B. Lorazo[18], M.J. Losty[7], J. Ludwig[10], A. Luig[10], A. Malik[21], M. Mannelli[8], S. Marcellini[2], C. Markus[3], A.J. Martin[13], J.P. Martin[18], G. Martinez[17], T. Mashimo[24], W. Matthews[25], P. Mättig[3], J. McKenna[29], E.A. Mckigney[15], T.J. McMahon[1], A.I. McNab[13], F. Meijers[8], S. Menke[3], F.S. Merritt[9], H. Mes[7], J. Meyer[27], A. Michelini[8], G. Mikenberg[26], D.J. Miller[15], R. Mir[26], W. Mohr[10], A. Montanari[2], T. Mori[24], M. Morii[24], U. Müller[3], B. Nellen[3], B. Nijjhar[16], S.W. O'Neale[1], F.G. Oakham[7], F. Odorici[2], H.O. Ogren[12], N.J. Oldershaw[16], C.J. Oram[28,a], M.J. Oreglia[9], S. Orito[24], M. Palazzo[2], J. Pálinkás[33], J.P. Pansart[21], J.R. Pater[16], G.N. Patrick[20], M.J. Pearce[1], P.D. Phillips[16], J.E. Pilcher[9], J. Pinfold[30], D.E. Plane[8], P. Poffenberger[28], B. Poli[2], A. Posthaus[3], T.W. Pritchard[13], H. Przysiezniak[30], D.L. Rees[1], D. Rigby[1], M.G. Rison[5], S.A. Robins[13], N. Rodning[30], J.M. Roney[28], E. Ros[8], A.M. Rossi[2], M. Rosvick[28], P. Routenburg[30], Y. Rozen[8], K. Runge[10], O. Runolfsson[8], D.R. Rust[12], R. Rylko[25], M. Sasaki[24], C. Sbarra[2], A.D. Schaile[8], O. Schaile[10], F. Scharf[3], P. Scharff-Hansen[8], P. Schenk[4], B. Schmitt[3], M. Schröder[8], H.C. Schultz-Coulon[10], M. Schulz[8], P. Schütz[3], J. Schwiening[3], W.G. Scott[20], M. Settles[12], T.G. Shears[16], B.C. Shen[4], C.H. Shepherd-Themistocleous[7], P. Sherwood[15], G.P. Siroli[2], A. Sittler[27], A. Skillman[15], A. Skuja[17], A.M. Smith[8], T.J. Smith[28], G.A. Snow[17], R. Sobie[28], S. Söldner-Rembold[10], R.W. Springer[30], M. Sproston[20], A. Stahl[3], M. Starks[12], C. Stegmann[10], K. Stephens[16], J. Steuerer[28], B. Stockhausen[3], D. Strom[19], F. Strumia[8], P. Szymanski[20], R. Tafirout[18], P. Taras[18], S. Tarem[26], M. Tecchio[8], N. Tesch[3], M.A. Thomson[8], E. von Törne[3], S. Towers[6], M. Tscheulin[10], T. Tsukamoto[24], E. Tsur[23], A.S. Turcot[9], M.F. Turner-Watson[8], P. Utzat[11], R. Van Kooten[12], G. Vasseur[21], P. Vikas[18], M. Vincter[28], E.H. Vokurka[16], F. Wäckerle[10], A. Wagner[27], D.L. Wagner[9], C.P. Ward[5], D.R. Ward[5], J.J. Ward[15], P.M. Watkins[1], A.T. Watson[1], N.K. Watson[7], P. Weber[6], P.S. Wells[8], N. Wermes[3],

B. Wilkens[10], G.W. Wilson[27], J.A. Wilson[1], T. Wlodek[26], G. Wolf[26], S. Wotton[11], T.R. Wyatt[16], S. Xella[2], G. Yekutieli[26], V. Zacek[18],

[1]School of Physics and Space Research, University of Birmingham, Birmingham B15 2TT, UK
[2]Dipartimento di Fisica dell' Università di Bologna and INFN, I-40126 Bologna, Italy
[3]Physikalisches Institut, Universität Bonn, D-53115 Bonn, Germany
[4]Department of Physics, University of California, Riverside CA 92521, USA
[5]Cavendish Laboratory, Cambridge CB3 0HE, UK
[6] Ottawa-Carleton Institute for Physics, Department of Physics, Carleton University, Ottawa, Ontario K1S 5B6, Canada
[7]Centre for Research in Particle Physics, Carleton University, Ottawa, Ontario K1S 5B6, Canada
[8]CERN, European Organisation for Particle Physics, CH-1211 Geneva 23, Switzerland
[9]Enrico Fermi Institute and Department of Physics, University of Chicago, Chicago IL 60637, USA
[10]Fakultät für Physik, Albert Ludwigs Universität, D-79104 Freiburg, Germany
[11]Physikalisches Institut, Universität Heidelberg, D-69120 Heidelberg, Germany
[12]Indiana University, Department of Physics, Swain Hall West 117, Bloomington IN 47405, USA
[13]Queen Mary and Westfield College, University of London, London E1 4NS, UK
[14]Technische Hochschule Aachen, III Physikalisches Institut, Sommerfeldstrasse 26-28, D-52056 Aachen, Germany
[15]University College London, London WC1E 6BT, UK
[16]Department of Physics, Schuster Laboratory, The University, Manchester M13 9PL, UK
[17]Department of Physics, University of Maryland, College Park, MD 20742, USA
[18]Laboratoire de Physique Nucléaire, Université de Montréal, Montréal, Quebec H3C 3J7, Canada
[19]University of Oregon, Department of Physics, Eugene OR 97403, USA
[20]Rutherford Appleton Laboratory, Chilton, Didcot, Oxfordshire OX11 0QX, UK
[21]CEA, DAPNIA/SPP, CE-Saclay, F-91191 Gif-sur-Yvette, France
[22]Department of Physics, Technion-Israel Institute of Technology, Haifa 32000, Israel
[23]Department of Physics and Astronomy, Tel Aviv University, Tel Aviv 69978, Israel
[24]International Centre for Elementary Particle Physics and Department of Physics, University of Tokyo, Tokyo 113, and Kobe University, Kobe 657, Japan
[25]Brunel University, Uxbridge, Middlesex UB8 3PH, UK
[26]Particle Physics Department, Weizmann Institute of Science, Rehovot 76100, Israel
[27]Universität Hamburg/DESY, II Institut für Experimental Physik, Notkestrasse 85, D-22607 Hamburg, Germany
[28]University of Victoria, Department of Physics, P O Box 3055, Victoria BC V8W 3P6, Canada
[29]University of British Columbia, Department of Physics, Vancouver BC V6T 1Z1, Canada
[30]University of Alberta, Department of Physics, Edmonton AB T6G 2J1, Canada
[31]Duke University, Dept of Physics, Durham, NC 27708-0305, USA
[32]Research Institute for Particle and Nuclear Physics, H-1525 Budapest, P O Box 49, Hungary
[33]Institute of Nuclear Research, H-4001 Debrecen, P O Box 51, Hungary

[a]Also at TRIUMF, Vancouver, Canada V6T 2A3
[b] Royal Society University Research Fellow
[c] Institute of Nuclear Research, Debrecen, Hungary

1 Introduction

The study of b quark fragmentation may help us understand more fully hadronization effects in non-perturbative QCD. From the point of view of perturbative QCD, the production of a heavy quark from a Z^0 decay is well understood. Measuring the B meson fragmentation function should help in determining the non-perturbative contribution and test the theoretical predictions for such effects [1]. The uncertainty in the b quark fragmentation is also a significant component of the error in many other heavy quark physics results which could be reduced by a more precise measurement of the fragmentation into B hadrons in Z^0 decays.

To date, most measurements of the fragmentation function have relied on the study of inclusive $B \to \ell X$ decays [2, 3], where ℓ is either an electron or a muon. These samples provide large statistics but have systematic limitations. With the high statistics now available at LEP, it has become possible to identify significant samples of $B \to \overline{D}\ell X$ or $B \to \overline{D}^*\ell X$ decays [4] in which the $\overline{D}$ or $\overline{D}^*$ is fully reconstructed. The kinematics of the $D^{(*)}\ell$ combination constrain the B energy more precisely than in inclusive $B \to \ell X$ decays. Therefore, in the absence of large statistics of fully reconstructed B mesons, the data samples used in this analysis are expected to provide the most direct opportunity for studying b quark fragmentation.

In this letter we use a maximum likelihood technique to extract information on the fragmentation function from the observed kinematics of $B \to D^{(*)}\ell X$ decays. Using this technique the models of Peterson *et al.* [5], Collins and Spiller [6], Kartvelishvili *et al.* [7] and Lund [8] are compared with the data. The sensitivity of the results to the fraction of B mesons originating from excited P-wave states is investigated. We also perform a model independent fit in order to extract the energy spectra of B^0 and B^+ mesons in Z^0 decays and compare this with theoretical predictions for the distribution.

Throughout this paper, charge conjugation is implicitly assumed and the symbol $D^{(*)}$ denotes either a D^0, D^+, $D^*(2010)^0$ or a $D^*(2010)^+$ meson. The symbol $D^{**}(B^{**})$ is used to denote a mixture of P-wave D(B) mesons.

2 Event Selection

A complete description of the OPAL detector can be found elsewhere [9]. Most of this analysis relies on the tracking of charged particles provided by the central detector, consisting of a silicon microvertex detector, a precision vertex drift chamber, a large volume jet chamber and chambers measuring the z coordinate[1] of tracks as they leave the jet chamber. The central detectors are surrounded by a magnet, outside which are electromagnetic and hadronic calorimeters which absorb and measure the energy of electrons, photons and hadrons. These are surrounded by muon chambers.

The data used in this analysis were recorded by OPAL from 1991 to 1994. They were collected from e^+e^- annihilations at centre of mass energies between 88.5 and 93.8 GeV. The selection criteria we used for isolating hadronic Z^0 decays are described elsewhere [10] and have an efficiency of $(98.4 \pm 0.4)\%$. After data quality and detector performance requirements, the available sample consists of 3.1 million events.

The selection of $B \to \overline{D}\ell^+X$ and $B \to \overline{D}^*\ell^+X$ events uses kinematic and vertex information from the decays of the B and D mesons. We consider the following five decay modes, $D^+ \to K^-\pi^+\pi^+$, $D^0 \to K^-\pi^+$, $D^0 \to K^-\pi^+\pi^+\pi^-$ and $D^{*+} \to D^0\pi^+$ where the D^0 decays to $K^-\pi^+$ or

[1]The OPAL coordinate system is defined with positive z along the e^- beam direction, θ and ϕ being the polar and azimuthal angles. The origin is taken to be the nominal interaction point.

$K^-\pi^+\pi^+\pi^-$ as before. The selection is described in detail in a previous paper [4] and is only summarized here.

Charged pions and kaons are identified using dE/dx information from the jet chamber. Electrons are identified from energy deposited in the electromagnetic calorimeter and dE/dx information from the jet chamber. Muons are identified by associating central detector tracks with track segments in the muon chambers along with loose dE/dx requirements to reject kaons and protons.

The $D^{(*)}$ mesons are selected by considering all track combinations consistent with the appropriate particle identification hypotheses. All $D^{(*)}\ell^-$ combinations are considered as possible B candidates. In selecting D^{*+} candidates we required the mass difference between the D^{*+} and D^0 candidate to be in the range 0.1415-0.1485 GeV. To ensure statistical independence, D^0 candidates were rejected if there existed a possible D^{*+} candidate with a mass difference less than 0.16 GeV.

To reduce the combinatorial background several kinematic cuts are made [4]; the main requirements being that the mass, $M_{D\ell}$, and energy, $E_{D\ell}$, of the candidates satisfy certain minimum criteria. The symbols $M_{D\ell}$ and $E_{D\ell}$ represent the invariant mass and the combined energy of the $D^{(*)}\ell$ system respectively and $x_{D\ell}$ is equal to $E_{D\ell}/E_{beam}$, where E_{beam} is the beam energy. We require the $D^{(*)}$ meson candidate to have energy greater than 5-9 GeV, depending on the decay channel, and place loose requirements on the decay lengths of the B and D meson candidates. To reject badly reconstructed vertices we require the lepton track and at least two of the D decay tracks to have at least one associated microvertex hit. This ensures that vertex reconstruction is dominated by tracks with microvertex detector information. The χ^2 for the vertex fit is required to be greater than 1%.

The mass distributions for the five different decay modes are shown in figure 1. A signal is clearly visible in each of the decay modes. Fitting the signal with a Gaussian and the background with a second order polynomial in each case gives a total of approximately 2300 signal events. The $K^-\pi^+$ mass distributions also show a satellite peak around 1.6 GeV which are also fitted with a Gaussian. An enhancement is expected in this region from partially reconstructed decays, particularly $D^0 \to K^-\rho^+, \rho^+ \to \pi^+\pi^0$, in which the π^0 is not reconstructed. These decays are not used for this analysis as the $D^{(*)}$ meson is not fully reconstructed. For the fragmentation fits we use the events within the mass region 1.805-1.925 GeV. To assess the background in the selected samples we used sidebands from the mass regions 1.735-1.795 GeV and 1.935-1.995 GeV.

In addition to the expected $B \to \overline{D}^{(*)}\ell^-X$ decays there are two other sources of $D^{(*)}\ell^-$ combinations which may contribute to the observed signals. These are from the decays $B \to D_s^{(*)}\overline{D}^{(*)}$ where the $D_s^{(*)}$ decay includes a lepton, and $B \to \overline{D}\tau X$ where the τ decays to either an electron or muon. These have been studied previously [4] and are estimated to make up 2-5% of our samples.

3 Monte Carlo Simulation

To model the $B \to \overline{D}^{(*)}\ell^+X$ decays we used a full Monte Carlo simulation of the OPAL detector [11]. The JETSET Monte Carlo program [12] was used to generate samples of semileptonic B decay events in each of the $\overline{D}^{(*)}\ell^+$ channels. The Peterson parameterization [5] was used for the b quark fragmentation, with the fragmentation parameter $\epsilon_b = 0.0057$ (corresponding to $\langle x_E \rangle = 0.691$) and we used the JETSET parameter $\Lambda_{LUND} = 0.31$ GeV [13]. The exclusive branching ratios used for these simulated events are described in detail in reference [14].

A significant fraction, f_{sl}^{**}, of semileptonic B decays are known to involve resonant $D^{(*)}\pi$ production [4, 15]. The states involved, generically referred to as D^{**}, are assumed to be saturated by the four P-wave mesons. Based on CLEO data [16] these decays were assumed to form 0.36 ± 0.12 of semileptonic B decays. Assuming the D^{**} decays are dominated by decays to $D^{(*)}\pi$ final states, isospin invariance was used to determine the fraction of decays yielding charged and neutral mesons. The fraction of D^{**} decays to $D^*\pi$ final states, p_v, was taken to be 0.54 ± 0.30 [14]. Semileptonic B decays may also result in non-resonant $D^{(*)}\pi$ production. These were not included in our standard simulations but have been studied using additional exclusive samples.

Similarly a significant fraction, $f_{\rm b}^{**}$, of b quarks are known to fragment to excited B^{**} mesons [17]. In analogy with the B decays to P-wave charmed mesons we assumed these were saturated by the P-wave mesons and that $f_{\rm b}^{**} = 0.36 \pm 0.12$. We also assumed the production rate of the two narrow P-wave B meson states are equal and twice the production rate of the two wide states [18]. For the studies without P-wave B mesons, where $f_{\rm b}^{**} = 0.0$ all the other Monte Carlo parameters were unchanged. The rate of direct B^* production was set such that $N(B^*)/N(B) \sim 0.75$ [19]. Due to the small mass difference between the B and B^* mesons, varying this parameter through its uncertainty causes a negligible effect on our results and is not considered as a systematic error.

As we use the Monte Carlo simulated data to obtain the reconstruction efficiencies for each decay channel, we need to be confident that they simulate the data well. We compared the simulated distributions of $E_{D\ell}$ and $M_{D\ell}$, on which the tightest selection cuts were made, with the same distributions from the data. It can be seen from figure 2 that the simulated distributions are in good agreement with the data.

4 Fragmentation Models

Experimentally we observe the B meson x_E distribution, where x_E is the energy of the weakly decaying B meson divided by the beam energy but, at present, there is no simple parameterization for this distribution. Instead all the commonly used theoretical parameterizations for heavy quark fragmentation use the non-observable variable z, where z is the fraction of the parton energy retained by the B hadron when the b quark undergoes hadronisation. We have studied these models in the context of the JETSET simulation and use the definition, $z = (E + p_{\|})_{hadron}/(E + p_{\|})_{available}$ [12], where most of the 'available' energy and momentum is from the b quark and $p_{\|}$ is the momentum in the direction of the quark momentum vector. Once the models have been compared with the data, these z distributions can then be used to predict the x_E distribution using a Monte Carlo simulation of the z to x_E mapping. It should be noted that this mapping has some sensitivity to the other parameters used when producing the Monte Carlo simulation, e.g. Λ_{LUND}. In this letter we study the following theoretical fragmentation functions:

Peterson *et al.* [5]

$$f(z) \propto z^{-1}\left(1 - \frac{1}{z} - \frac{\epsilon_{\rm b}}{(1-z)}\right)^{-2}$$

where $\epsilon_{\rm b}$ is expected to vary as the inverse square of the effective quark mass, M_{quark}^{-2};

Collins and Spiller [6]

$$f(z) \propto \left(\frac{(1-z)}{z} + \frac{(2-z)\tilde{\epsilon_{\rm b}}}{(1-z)}\right)(1+z^2)\left(1 - \frac{1}{z} - \frac{\tilde{\epsilon_{\rm b}}}{(1-z)}\right)^{-2}$$

where $\tilde{\epsilon_{\rm b}}$ is also expected to vary as M_{quark}^{-2};
Kartvelishvili *et al.* [7]

$$f(z) \propto z^{\alpha_{\rm b}}(1-z)$$

and Lund [8]

$$f(z) \propto \frac{1}{z}(1-z)^a exp\left(-\frac{bM_T^2}{z}\right)$$

where bM_T^2 is considered as a free parameter and a is a universal parameter which has been tuned to 0.18 by OPAL [13]. The general symbol ε is used in this paper to describe the free parameters in the models ($\epsilon_{\rm b}$, $\tilde{\epsilon_{\rm b}}$, $\alpha_{\rm b}$ or bM_T^2 respectively).

5 Fit Method

To fit the z distributions predicted by our models to the data, we first have to consider the measurable kinematics of the decays and how they are related to z. There is an approximately linear relationship between $\langle x_E \rangle$ for a B hadron and $\langle z \rangle$. We therefore expect a strong correlation between the scaled energy of the reconstructed decay products of the B hadron, x_{Dl}, and z. Unfortunately using only the energy of the decay products to determine the z distribution would be very dependent on the Monte Carlo modelling of the decay kinematics due to the missing neutrino. Consequently we also consider the invariant mass of the reconstructed decay products, M_{Dl}, which is correlated with the neutrino energy. This results in a fitting technique less dependent on the Monte Carlo model.

Using the Monte Carlo data samples described in section 3, we produced a matrix which, for an event within a given bin of z, gave the probability, $\boldsymbol{\mathcal{P}}(M_{Dl}, x_{Dl}|z)$, of that event being in a certain bin of M_{Dl} and x_{Dl}. In this paper we used 2 M_{Dl} bins, 5 x_{Dl} bins and 8 z bins. This matrix, produced using large samples of Monte Carlo events without detector simulation, was scaled by the reconstruction efficiency for each (M_{Dl},x_{Dl}) bin, calculated using independent samples of Monte Carlo data with a full detector simulation. The matrix was then normalized to sum to one over each z bin.

Before fitting we divided the data into M_{Dl} and x_{Dl} bins to produce an array, $\boldsymbol{\mathcal{D}}(M_{Dl}, x_{Dl})$. We then split the data from the sideband regions into an array, $\boldsymbol{\mathcal{B}}(M_{Dl}, x_{Dl})$, with the same binning as the data array. The expected background in each (M_{Dl}, x_{Dl}) bin due to $\mathrm{B} \to \overline{\mathrm{D}}\tau\mathrm{X}$ and $\mathrm{B} \to \mathrm{D}_{\mathrm{s}}^{(*)}\overline{\mathrm{D}}^{(*)}$ decays was also added to the array $\boldsymbol{\mathcal{B}}(M_{Dl}, x_{Dl})$, which was then normalized to sum to one. We then fitted to the free parameter, ε, in our chosen fragmentation function by maximizing with respect to ε the log likelihood:

$$\boldsymbol{\mathcal{L}} = \sum_{channels} \sum_{M,x} \boldsymbol{\mathcal{D}}(M_{Dl}, x_{Dl}) \times \ln\{P_{sig} \times \sum_{z} \mathbf{f}(z,\varepsilon) \times \boldsymbol{\mathcal{P}}(M_{Dl}, x_{Dl}|z) + (1 - P_{sig}) \times \boldsymbol{\mathcal{B}}(M_{Dl}, x_{Dl})\}$$

where $\mathbf{f}(z,\varepsilon)$ was the integral of our chosen fragmentation function over the z-bin (normalized to sum to one over all the z-bins) and P_{sig} was the fraction of events in our D mass window that are signal.

There is a small model dependence in the fit due to the fragmentation model used to produce the Monte Carlo samples from which we obtained $\boldsymbol{\mathcal{P}}(M_{Dl}, x_{Dl}|z)$. To reduce this dependence,

for each model, we used the predicted z distribution from the fit to produce a new probability matrix and repeated the fit to the data. In principle repeating this procedure many times would remove any Monte Carlo fragmentation model dependence from the fit. As the fragmentation model used to produce our Monte Carlo samples was already a reasonable description of the data, we found the results converged after one iteration.

The fit was tested on many Monte Carlo samples of data produced using Peterson fragmentation with various values of ϵ_b. In all cases the fit result was consistent with the value of ϵ_b used to create the sample. In order to check that the statistical errors produced by the fit were reasonable, we produced many samples of simulated data with the same value of ϵ_b and fitted them all individually. The width of the distribution of results from these fits was consistent with the typical statistical error.

For the model independent fit to the B meson x_E distribution we performed a similar fit to that described above, but instead of using z in the probability matrix we split the x_E distribution into bins to produce a matrix $\mathcal{P}(M_{Dl}, x_{Dl}|x_E)$. We then maximized the log likelihood above replacing $\mathbf{f}(z, \varepsilon)$ by a free parameter for all but one of the x_E bins and the summation over z bins was changed to be over x_E bins. The last x_E bin was used to normalize the fit, whereby $x_{last} = 1 - \Sigma x_i$, and was therefore not a free parameter. Due to the high degree of bin to bin correlation in this fit, with the present statistics, we only fit to four x_E bins.

6 Results

We performed two sets of fits to the data using the fragmentation models. Firstly using Monte Carlo samples without P-wave B mesons (f_b^{**}=0.0) and secondly using Monte Carlo samples including P-wave B mesons ($f_b^{**} = 0.36$). The results of the fits to the four fragmentation models are shown in table 1, from which one can see how the inclusion of these higher spin states affects our results. The z distributions predicted by the results of the fits including the P-wave B mesons are shown in figure 3a. To obtain the relevant x_E distribution we reweighted the z distribution from a Monte Carlo sample to the fitted fragmentation function. Figure 3b illustrates the x_E distributions obtained from the fit results compared with OPAL data. For this comparison, the data were corrected using a matrix $\mathcal{Q}(M_{Dl}, x_{Dl}|x_E)$ which represents the probabilities that an event observed in a given (M_{Dl}, x_{Dl}) bin originated from each x_E bin. This matrix was constructed in the same way as $\mathcal{P}(M_{Dl}, x_{Dl}|x_E)$, but normalized so that the sum over x_E for each (M_{Dl}, x_{Dl}) bin was unity. The Peterson fragmentation model was used to obtain the central values, while the other fitted models were used in estimating the systematic errors. The predicted x_E distributions for all four models are in satisfactory agreement with the data.

It can be seen from the results in table 1 that including P-wave mesons in our simulation does affect the fit to the theoretical z distribution, and results in the prediction of a fragmentation function with a higher $\langle z \rangle$. This is expected as the parameter, z, describes the energy distribution of the B hadron produced when the b quark hadronises, the 'first rank' hadron. Inclusion of the P-wave mesons in the simulations allow extra, more energetic, species for such hadrons. As a result the first rank hadrons in the simulations must be more energetic to produce the same decay product energy distributions. Using our Monte Carlo simulations we determined the shift between the mean scaled energy for the first rank hadrons, $\langle x'_E \rangle$, and for the weakly decaying mesons, $\langle x_E \rangle$. For $f_b^{**} = 0.0(0.36)$ we found $\Delta\langle x_E \rangle = 0.005(0.027)$. As expected the fitted mean scaled energy for the weakly decaying B mesons, $\langle x_E \rangle$, is insensitive to the inclusion of the P-wave mesons.

	without B^{**}		with B^{**}		Systematic
Model	Fit Result (ε)	$\langle x_E \rangle$	Fit Result (ε)	$\langle x_E \rangle$	Error
Peterson	$(4.7^{+1.0}_{-0.8}) \times 10^{-3}$	$0.694^{+0.006}_{-0.005}$	$(2.4^{+0.6}_{-0.5}) \times 10^{-3}$	$0.695^{+0.006}_{-0.006}$	$^{+0.003}_{-0.004}$
C. and S.	$(2.5^{+1.0}_{-0.7}) \times 10^{-3}$	$0.683^{+0.006}_{-0.005}$	$(6.4^{+3.9}_{-2.7}) \times 10^{-4}$	$0.684^{+0.006}_{-0.006}$	$^{+0.003}_{-0.003}$
Kart.	$(10.0^{+0.9}_{-0.8})$	$0.697^{+0.006}_{-0.007}$	$(13.5^{+1.5}_{-1.3})$	$0.699^{+0.007}_{-0.006}$	$^{+0.003}_{-0.003}$
Lund	$(5.3^{+0.6}_{-0.5})$	$0.702^{+0.006}_{-0.006}$	$(7.5^{+1.0}_{-0.8})$	$0.703^{+0.006}_{-0.006}$	$^{+0.003}_{-0.003}$

Table 1: Fit results and derived result for $\langle x_E \rangle$ for the four different fragmentation functions with and without P-wave B mesons in the Monte Carlo simulation. The errors shown with the results are the statistical errors from the maximum likelihood fit. The systematic errors shown in the final column are described below in section 7 and are approximately equal for the fits with and without the P-wave B mesons.

	without B^{**}		with B^{**}	
Model	χ^2	Probability	χ^2	Probability
Peterson	24.91	35.5%	23.59	42.7%
Collins and Spiller	24.67	36.8%	23.45	43.5%
Kartvelishvili	28.42	20.0%	26.10	29.6%
Lund	24.86	35.8%	23.83	41.3%

Table 2: A comparison of the χ^2 and derived fit probability calculated from the predicted x_{Dl} distributions for the four fragmentation models. For each model the number of degrees of freedom used to calculate the probability was 23.

As another check of our fit and as a method of comparing the different fragmentation models, the results given in table 1 were used with the fit probability densities to predict the data x_{Dl} distributions for D^+, D^0 and D^{*+} events in each mass bin, where the probability density for each x_{Dl} bin was :

$$\sum_{z-bins} \mathbf{f}(z,\varepsilon) \times \mathcal{P}(M_{Dl}, x_{Dl}|z).$$

The calculated χ^2 and corresponding probabilities for the agreement of each model with the normalized data x_{Dl} distributions are listed in table 2. For all four models the x_{Dl} distributions predicted by our results were in satisfactory agreement with the data. Figure 4 shows the predicted distributions from the Collins and Spiller fit including the P-wave B mesons compared with the background subtracted data distributions.

The model independent fit to the x_E distribution is shown in figure 5a where the errors shown are statistical only. The distribution is compared with the predicted x_E distributions for the four models. The predicted distributions for all four models are reasonably consistent with the result of this free fit. Due to the large bin to bin correlations in this fit, the statistical errors are quite large. From this distribution and a Monte Carlo simulation to estimate the fraction of data below $x_E = 0.2$ we derive $\langle x_E \rangle = 0.72 \pm 0.05$ where the error is statistical only. The results of this fit and the correlation matrix are shown in table 3.

Bin	x_E Range	Fit Result	Correlation Matrix			
			Bin 1	Bin 2	Bin 3	Bin 4
1	0.2 - 0.5	0.099 ± 0.015	1.00	-0.60	0.28	-0.21
2	0.5 - 0.7	0.170 ± 0.041		1.00	-0.79	0.38
3	0.7 - 0.85	0.442 ± 0.071			1.00	-0.84
4	0.85 - 1.0	0.289 ± 0.039				1.00

Table 3: Results of model independent fit to four x_E bins and the bin to bin correlations. The errors for the fit results presented are statistical only.

In figure 5b we compare the model independent fit to a theoretical prediction for the B^0/B^+ energy spectra. This prediction is described in full elsewhere [1] and only a summary is presented here. In this theory the perturbative contribution to the fragmentation function [20] is convolved with a parameterization for non-perturbative effects of the following form:

$$f^{np}(x_E) = A(1 - x_E)^{\alpha} x_E^{\beta}$$

where A is a normalization factor. The values of α and β for c quark fragmentation were obtained [1] by fitting to the D^0 fragmentation function measured by ARGUS [21]. Assuming that the perturbative matching scale, $\mu_0 = M_b = 4.5$ GeV, $\Lambda_{QCD} = 300(200)$ MeV for five quark flavours and that non-perturbative effects scale linearly in the mass of the heavy quark the values $\alpha_B = 1.46(0.595)$ and $\beta_B = 37.76(18.67)$ were obtained [1]. The other fragmentation models used in this analysis are constrained by OPAL data whereas this theory has many free parameters and systematic uncertainties. Nevertheless the predicted distribution shown is in good agreement[2] with our data where $\chi^2 = 1.62$ for $\Lambda_{QCD} = 300$ MeV and $\chi^2 = 6.17$ for $\Lambda_{QCD} = 200$ MeV with 3 degrees of freedom.

7 Systematic Uncertainties

There are several sources of systematic uncertainty which affect our results, most of which are due to uncertainties in the Monte Carlo modelling of the decay channels. These are summarized in table 4 and were evaluated as follows:

- Although $f_{\rm b}^{**}$ has been measured [17] there are still large uncertainties in the fraction of wide P-wave states. As a result we use a uncertainty of ± 0.12 which is larger than the measured errors. This error was evaluated by producing new samples of generator level Monte Carlo with $f_{\rm b}^{**}$ scaled accordingly and repeating the fit. As can be seen from the difference in the results shown in table 1 varying $f_{\rm b}^{**}$ has a large effect on the free parameters of the models, ε, but the fitted value of $\langle x_E \rangle$ is much less sensitive.

- We varied f_{sl}^{**} by ± 0.12 as measured by CLEO [16]. By splitting the Monte Carlo samples into the components from D^{**}, D^* and direct decays and recombining them scaled according to the variation in f_{sl}^{**} to produce a new probability matrix, $\mathcal{P}(M_{Dl}, x_{Dl}|z)$, we refit the data and obtained the systematic uncertainty.

- The uncertainty due to p_v was evaluated in the same way as for f_{sl}^{**} whereby p_v was varied by ± 0.30 as assumed previously [14].

[2] In the comparison with the model independent fit, extra complications to the theory such as the P-wave B mesons are ignored.

Systematic	Peterson	C. and S.	Kart.	Lund
	$\Delta\langle x_E\rangle \times 10^3$			
$f_{\rm b}^{**} \pm 0.12$	$+0.1$ -0.5	$+0.3$ -0.7	$+0.2$ -0.5	$+0.3$ -0.4
$f_{sl}^{**} \pm 0.12$	$+1.5$ -2.8	$+1.8$ -2.4	$+2.3$ -2.5	$+1.8$ -2.4
$p_v \pm 0.3$	$+2.0$ -1.9	$+1.5$ -1.5	$+1.5$ -1.5	$+1.7$ -1.4
Non-resonant decays (10%)	$+1.3$	$+1.2$	$+1.5$	$+1.5$
$\rm B \to \overline{D}\tau X$ and $\rm B \to D_s^{(*)}\overline{D}^{(*)}$ background	$+0.5$ -0.8	$+0.5$ -0.7	$+0.6$ -0.7	$+0.6$ -0.7
Combinatorial background	$+0.5$ -0.6	$+0.5$ -0.7	$+0.5$ -0.5	$+0.4$ -0.5
Total	$+2.9$ -3.6	$+2.7$ -3.1	$+3.2$ -3.1	$+3.0$ -3.0

Table 4: Effect on $\langle x_E\rangle$ of the systematic errors for the four different fragmentation fits.

- Experimental measurements indicate that a large fraction of the $\rm D^{**}$ component of semileptonic B decays consist of the P-wave states [4]; but a contribution of non-resonant decays of the type $\rm B \to D^{(*)}\ell\nu\pi$ is not excluded at the 10% level. Therefore to account for the possibility of such decays we produced Monte Carlo data samples in which 10% of the semileptonic B decays were of this type. Fitting to the data using these samples to produce the probability matrix we estimated the uncertainty due to such decays.

- The systematic uncertainty due to background from $\rm B \to \overline{D}\tau X$ and $\rm B \to D_s^{(*)}\overline{D}^{(*)}$ decays was assessed by varying the measured branching ratios[3] by their uncertainty.

- The uncertainty in the $M_{\rm D\ell}$ and $E_{\rm D\ell}$ distributions from the sideband regions was evaluated by moving the sideband regions by 30 MeV in both directions and the effect on the fit result was used as the systematic error.

For all four models, both the statistical and systematic errors are fully correlated. Therefore to combine them we took the mean of the four results and errors for the fits including the P-wave B mesons shown in table 1. In combining these results an extra systematic error due to the model dependence was included. This was calculated as the r.m.s. of the deviation from the mean of the individual results. This gives a final result for $\langle x_E\rangle$:

$$\langle x_E\rangle = 0.695 \pm 0.006 \pm 0.003 \pm 0.007$$

where the errors are statistical, systematic and model dependence respectively.

8 Conclusions

Using a sample of approximately 2300 semileptonic $\rm B^0/B^+$ meson decays to charm mesons we have fitted the data to four theoretical models for the b quark fragmentation variable z. Using

[3]We used the branching ratios $B(\rm b \to D\tau X) = (4.1 \pm 1.0)\%$ and $B(\rm B \to D_s^{(*)}\overline{D}^{(*)}) = (5.0 \pm 0.9)\%$ [22].

these results, we obtained the mean B^0/B^+ meson energy fraction :

$$\langle x_E \rangle = 0.695 \pm 0.006 \pm 0.003 \pm 0.007,$$

where the errors are statistical, systematic and model dependence respectively. With the statistics available, none of the models can be excluded and the quality of the fit is unchanged by including the P-wave B mesons in the data simulation.

This result is in good agreement with previous measurements [2, 3, 23] with a small improvement in precision. It is also consistent with a less precise result using a similar method and event sample [24]. We emphasize that in this paper $\langle x_E \rangle$ refers to the weakly decaying hadron rather than the first-rank hadron. Using $\Delta\langle x_E \rangle$ as predicted by the JETSET model we can translate this result to the corresponding mean energy fraction for the first rank hadrons, $\langle x'_E \rangle$. For $f_b^{**} = 0.0$ and 0.36 we obtain $\langle x'_E \rangle = 0.700$ and $\langle x'_E \rangle = 0.722$ respectively.

We have also made the first model independent fit to the shape of the x_E distribution for weakly decaying B mesons. This fit is consistent with the predicted distributions from the four fragmentation models studied and with the present statistics none of them can be eliminated. In addition, the fit is in good agreement with a theoretical prediction for the B meson energy spectrum.

Acknowledgements

We thank Paolo Nason for useful discussion and providing the program from which we produced the theoretical x_E distribution shown in figure 5b.

It is a pleasure to thank the SL Division for the efficient operation of the LEP accelerator, the precise information on the absolute energy, and their continuing close cooperation with our experimental group. In addition to the support staff at our own institutions we are pleased to acknowledge the

Department of Energy, USA,
National Science Foundation, USA,
Particle Physics and Astronomy Research Council, UK,
Natural Sciences and Engineering Research Council, Canada,
Fussefeld Foundation,
Israel Ministry of Science,
Israel Science Foundation, administered by the Israel Academy of Science and Humanities,
Minerva Gesellschaft,
Japanese Ministry of Education, Science and Culture (the Monbusho) and a grant under the Monbusho International Science Research Program,
German Israeli Bi-national Science Foundation (GIF),
Direction des Sciences de la Matière du Commissariat à l'Energie Atomique, France,
Bundesministerium für Forschung und Technologie, Germany,
National Research Council of Canada,
A.P. Sloan Foundation and Junta Nacional de Investigação Científica e Tecnológica, Portugal.
Hungarian Foundation for Scientific Research, OTKA T-016660.

References

[1] G. Colangelo and P. Nason, *Phys. Lett.* **B285** (1992) 167.

[2] OPAL Collaboration, P. D. Acton *et al.*, *Z. Phys.* **C58** (1993) 523.

[3] ALEPH Collaboration, D. Decamp *et al.*, *Phys. Lett.* **B244** (1990) 551;
DELPHI Collaboration, P. Abreu *et al.*, *Z. Phys.* **C56** (1992) 47;
L3 Collaboration, B. Adeva *et al.*, *Phys. Lett.* **B241** (1990) 416;
L3 Collaboration, B. Adeva *et al.*, *Phys. Lett.* **B271** (1991) 461;
OPAL Collaboration, M. Z. Akrawy *et al.*, *Phys. Lett.* **B263** (1991) 311.

[4] OPAL Collaboration, R. Akers *et al.*, *Z. Phys.* **C67** (1995) 57.

[5] C. Peterson, D. Schlatter, I. Schmitt and P. M. Zerwas, *Phys. Rev.* **D 27** (1983) 105.

[6] P. Collins and T. Spiller, *J. Phys.* **G11** (1985) 1289.

[7] V. G. Kartvelishvili, A. K. Likhoded and V. A. Petrov, *Phys. Lett.* **B78** (1978) 615.

[8] B. Andersson, G. Gustafson and B. Söderberg, *Z. Phys.* **C20** (1983) 317.

[9] OPAL Collaboration, K. Ahmet *et al.*, *Nucl. Instrum. Methods* **A305** (1991) 275;
P. P. Allport *et al.*, *Nucl. Instrum. Methods* **A324** (1993) 34;
P. P. Allport *et al.*, *Nucl. Instrum. Methods* **A346** (1994) 476.

[10] OPAL Collaboration, G. Alexander *et al.*, *Z. Phys.* **C52** (1991) 175.

[11] J. Allison *et al.*, *Nucl. Instrum. Methods* **A317** (1992) 47.

[12] T. Sjöstrand, *Comp. Phys. Comm.* **39** (1986) 347;
T. Sjöstrand and M. Bengtsson, *Comp. Phys. Comm.* **43** (1987) 367.

[13] OPAL Collaboration, M. Z. Akrawy *et al.*, *Z. Phys.* **C47** (1990) 505.

[14] OPAL Collaboration, P. D. Acton *et al.*, *Phys. Lett.* **B307** (1993) 247.

[15] ARGUS Collaboration, H. Albrecht *et al.*, *Z. Phys.* **C57** (1993) 533;
ALEPH Collaboration, D. Buskulic *et al.*, *Phys. Lett.* **B345** (1995) 103.

[16] CLEO Collaboration, R. Fulton *et al.*, *Phys. Rev.* **D43** (1991) 651.

[17] OPAL Collaboration, R. Akers *et al.*, *Z. Phys.* **C66** (1995) 19;
DELPHI Collaboration, P. Abreu *et al.*, *Phys. Lett.* **B345** (1995) 598.

[18] E. J. Eichten, C. T. Hill and C. Quigg, *Phys. Rev. Lett.* **71** (1993) 4116.

[19] DELPHI Collaboration, P. Abreu *et al.*, 'B* Production in Z^0 Decays', CERN-PPE/95-53;
L3 Collaboration, M. Acciarri *et al.*, *Phys. Lett.* **B345** (1995) 589.

[20] B. Mele and P. Nason, *Phys. Lett.* **B245** (1990) 635;
B. Mele and P. Nason, *Nucl. Phys.* **B361** (1991) 626.

[21] ARGUS Collaboration, H. Albrecht *et al.*, *Z. Phys.* **C52** (1991) 353.

[22] Particle Data Group, L. Montanet *et al.*, *Phys. Rev.* **D50** (1994).

[23] L3 Collaboration, O. Adriani *et al.*, *Phys. Lett.* **B288** (1992) 412.

[24] DELPHI Collaboration, P. Abreu *et al.*, *Z. Phys.* **C57** (1993) 181.

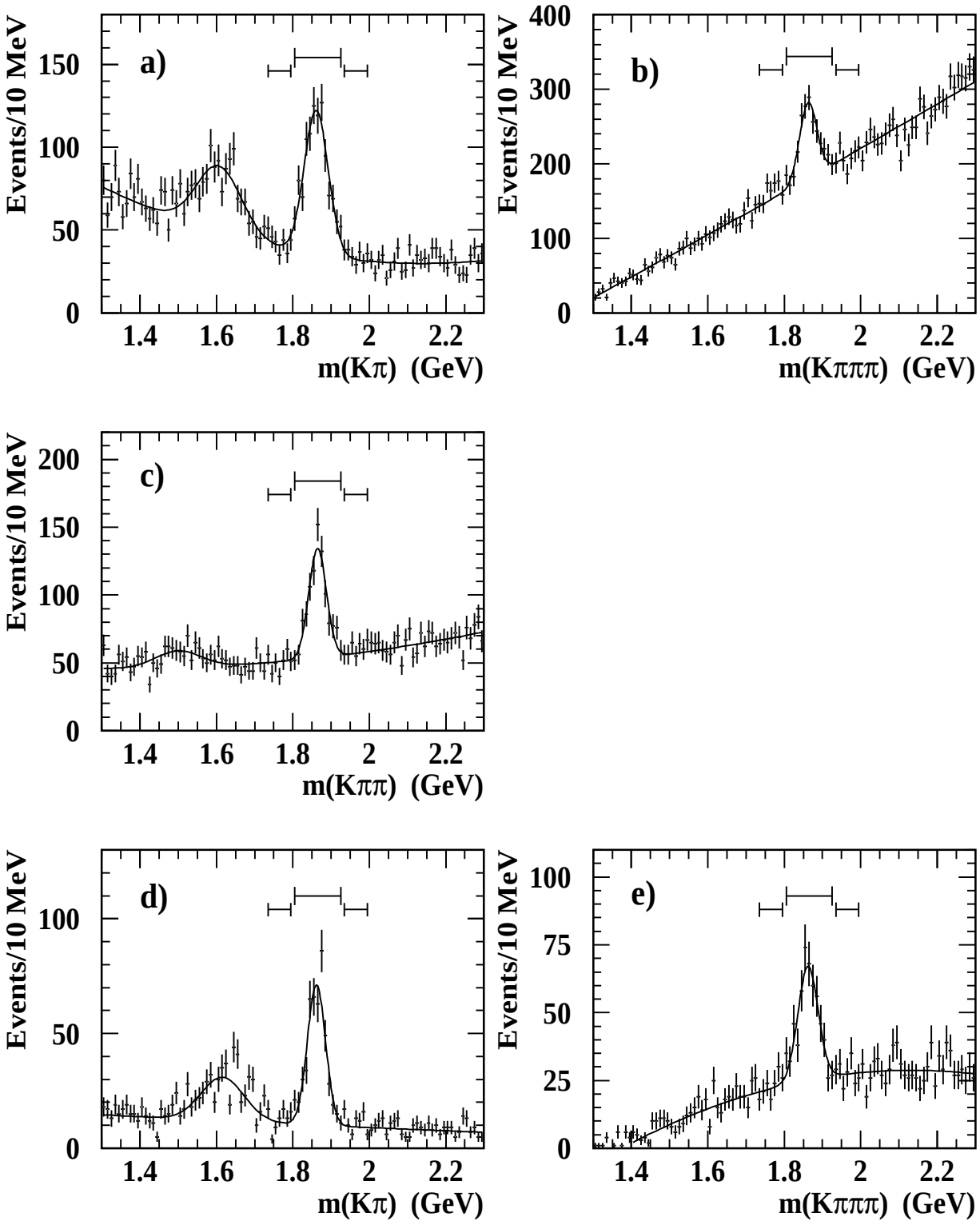

Figure 1: D mass distributions for a) $D^0 \to K^-\pi^+$ events, b) $D^0 \to K^-\pi^+\pi^+\pi^-$ events, c) $D^+ \to K^-\pi^+\pi^+$ events, d) $D^{*+} \to D^0\pi^+$, $D^0 \to K^-\pi^+$ events and e) $D^{*+} \to D^0\pi^+$, $D^0 \to K^-\pi^+\pi^+\pi^-$ events. The fits shown are the sum of Gaussians and second order polynomials and the lines above the peaks mark the signal and sideband regions.

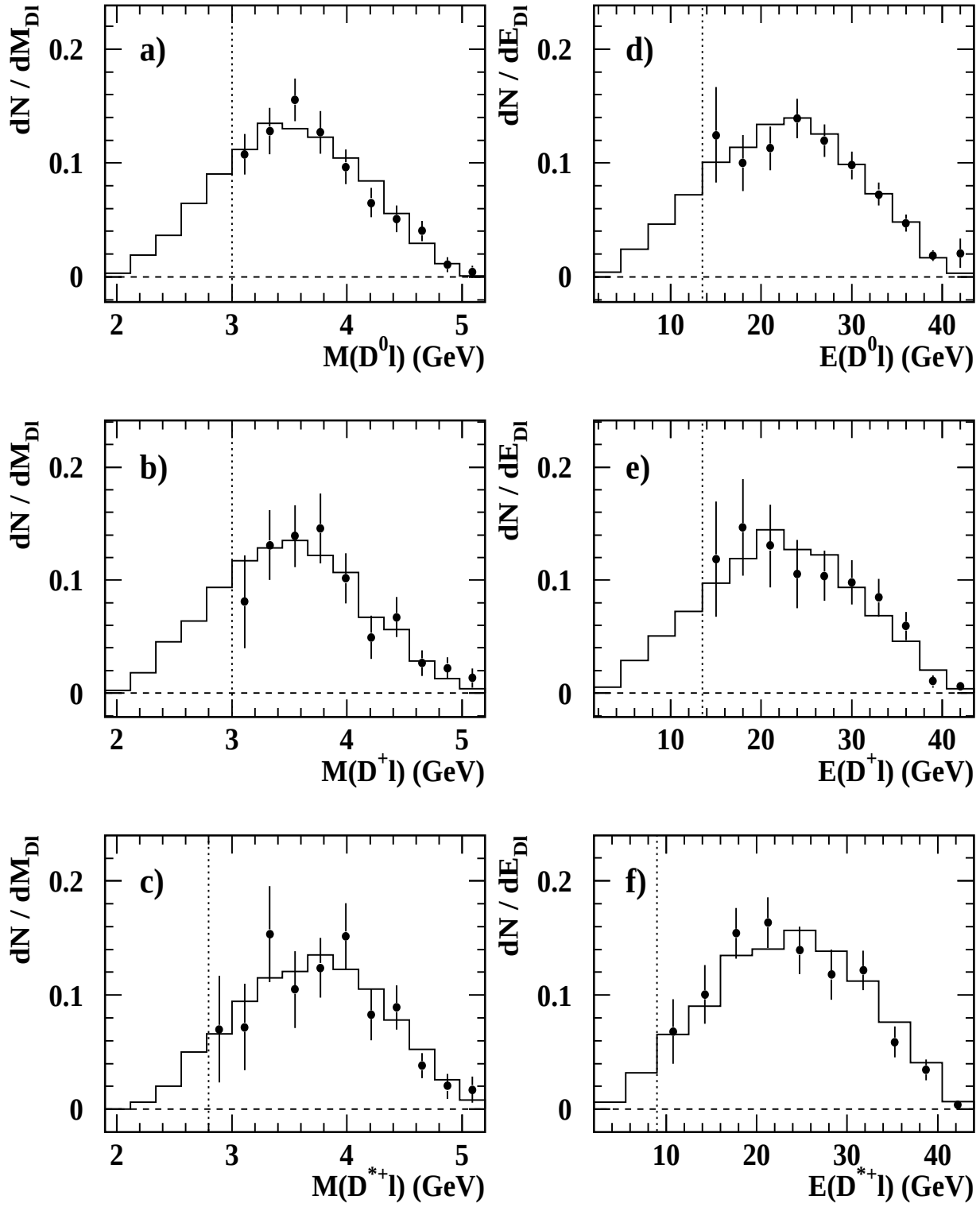

Figure 2: Monte Carlo and data comparison of $M_{\mathrm{D}\ell}$ for a) $\mathrm{b} \to \mathrm{D}^0\ell\mathrm{X}$ events, b) $\mathrm{b} \to \mathrm{D}^+\ell\mathrm{X}$ events and c) $\mathrm{b} \to \mathrm{D}^{*+}\ell\mathrm{X}$ events and $E_{\mathrm{D}\ell}$ for d) $\mathrm{b} \to \mathrm{D}^0\ell\mathrm{X}$ events, e) $\mathrm{b} \to \mathrm{D}^+\ell\mathrm{X}$ events and f) $\mathrm{b} \to \mathrm{D}^{*+}\ell\mathrm{X}$ events. The histograms are the generator level Monte Carlo distributions and the points are efficiency corrected data after background subtraction. The dotted line on each plot indicates the experimental lower limit due to the selection criteria applied. These distributions are not fitted, only normalized such that the integration over the experimental ranges are equal.

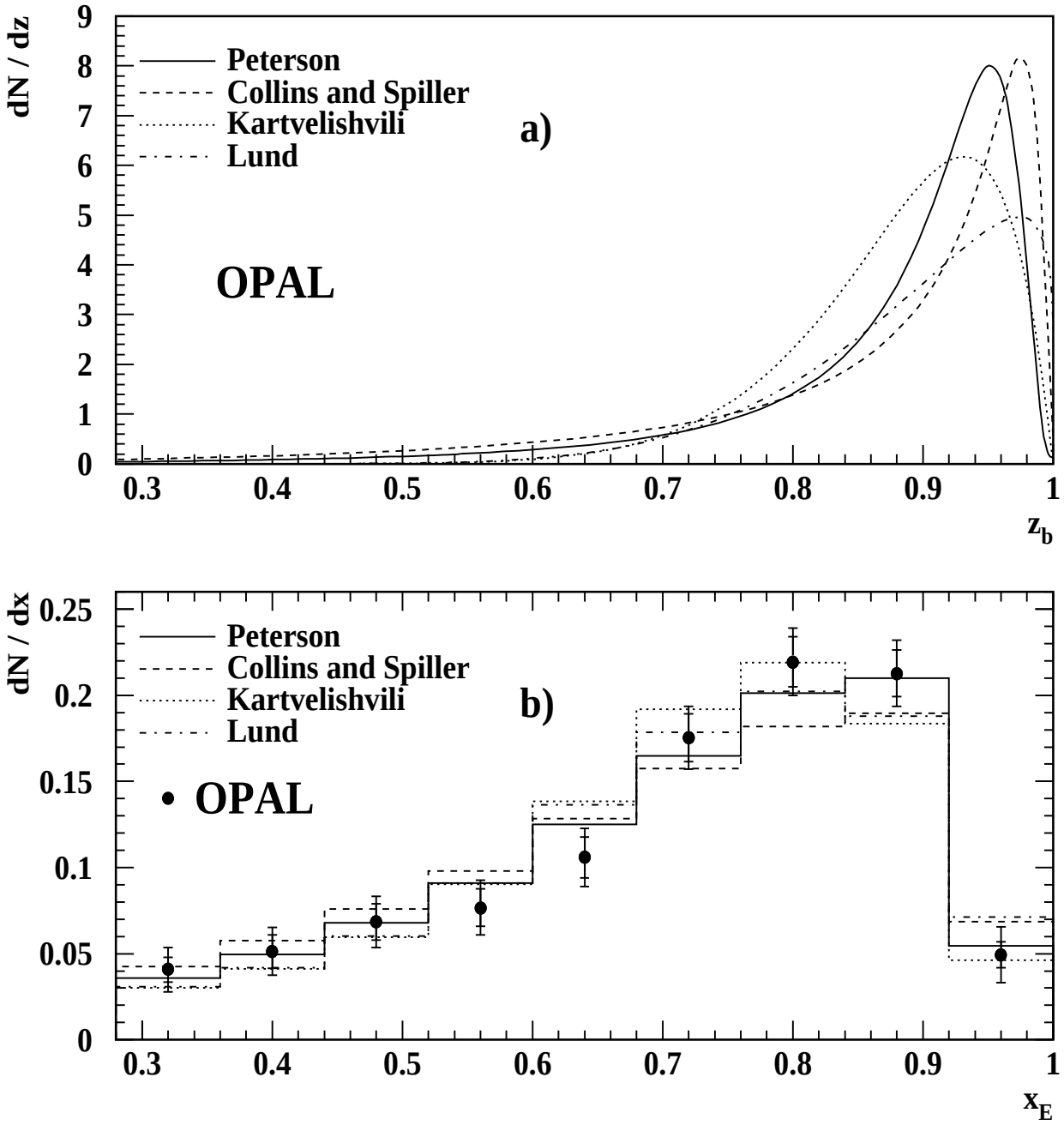

Figure 3: a) Normalized fit results for the four fragmentation functions with the free parameters set to the values given in table 1 (results for fits with P-wave B mesons). b) Distribution to illustrate the fit results in terms of x_E. The points are the OPAL data unfolded using the Peterson fragmentation model and the histograms are the predicted x_E distributions from our four model dependent fit results. The smaller errors on the points are the statistical errors and the larger are the sum of the statistical errors and the systematic errors (including an error due to the model dependence).

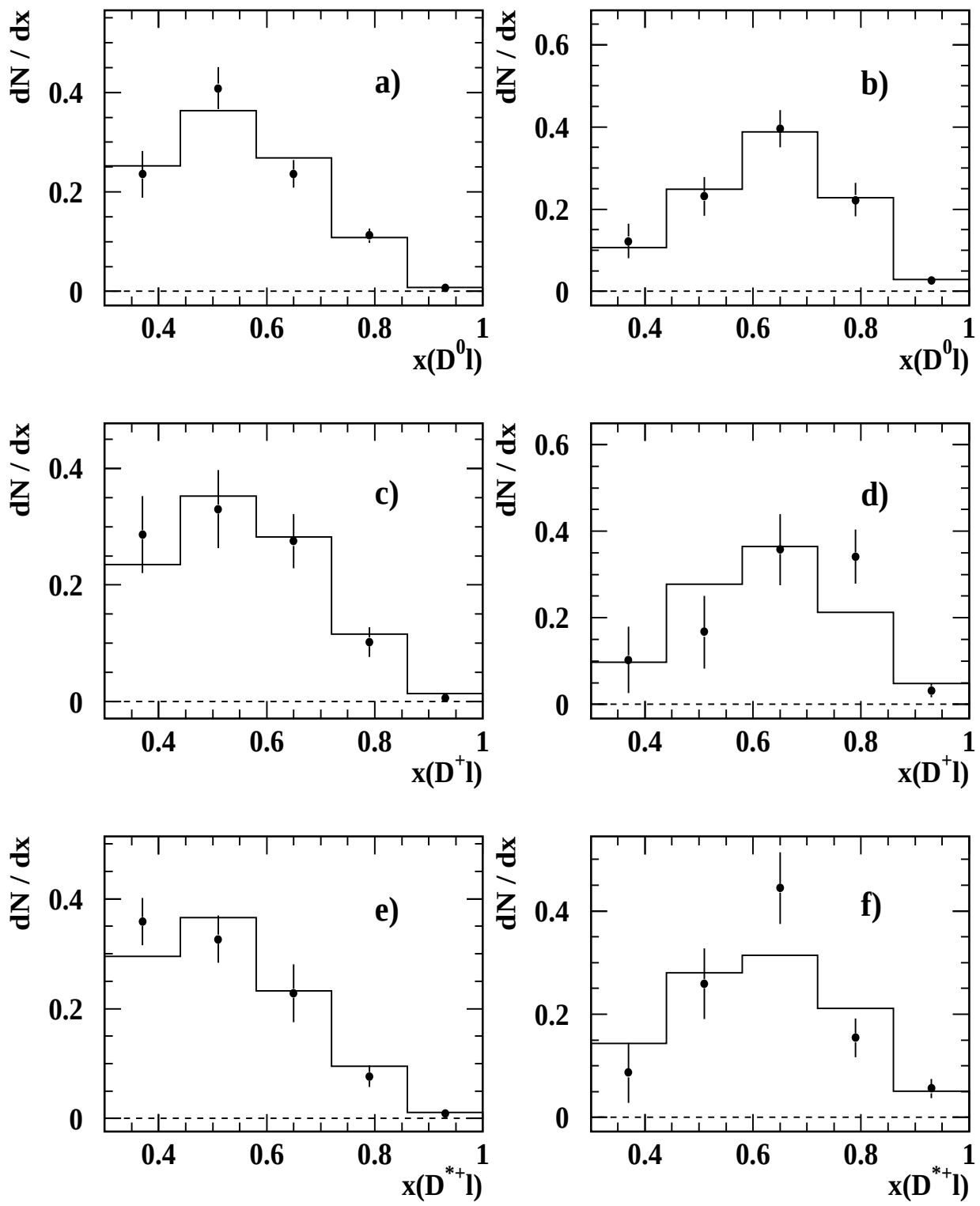

Figure 4: Comparison of data $x_{\mathrm{D}\ell}$ distributions with predicted distributions for each $M_{\mathrm{D}\ell}$ bin from the Collins and Spiller fit result for a) and b) b $\rightarrow$ $\mathrm{D}^0\ell$X events, c) and d) b $\rightarrow$ $\mathrm{D}^+\ell$X events and e) and f) b $\rightarrow$ $\mathrm{D}^{*+}\ell$X events. Histograms a), c) and e) are for the lower $M_{\mathrm{D}\ell}$ bin (3.0 - 4.0 GeV) and b), d) and f) for the higher $M_{\mathrm{D}\ell}$ bin (4.0 - 5.0 GeV). The histograms are the predicted distributions and the points are the background subtracted data distributions.

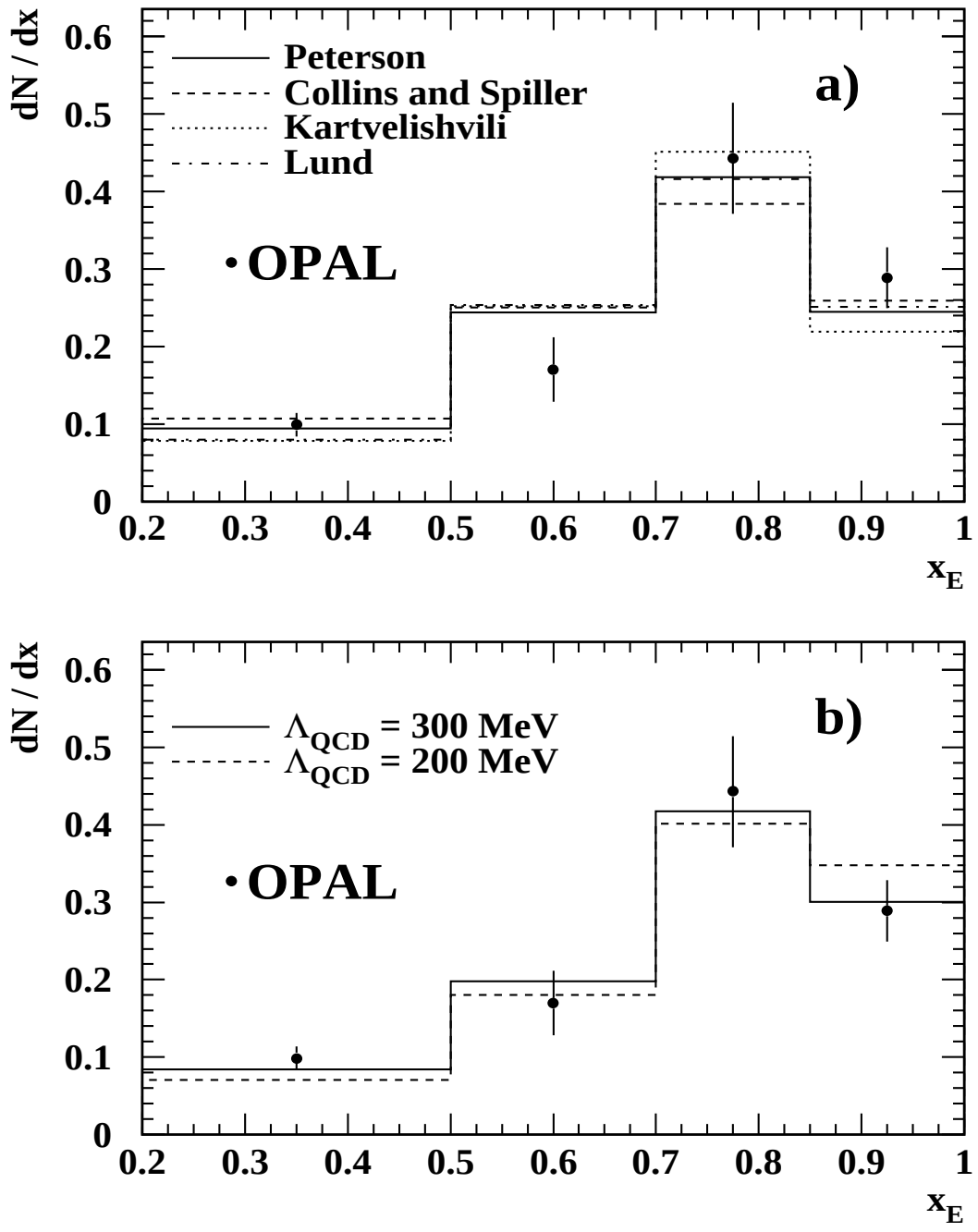

Figure 5: Comparison of model independent binned fit to x_E distribution with all the bin to bin correlations accounted for in the fit, shown by the points (the errors shown being statistical only), with histograms showing a) the predicted x_E distributions from our parameterized fits to the four models and b) the theoretically predicted x_E distributions for Λ_{QCD} = 200 MeV and 300 MeV.